P8R.2 **COMPARISON OF THE NEXRAD LEGACY AND LINCOLN LABORATORIES ECHO TOPS PRODUCTS**

Thomas A. Seliga*, Allen D. Mackey, Michael D. West and James Hill
Volpe National Transportation Systems Center, Cambridge, MA
Danny Sims and Ved Sud
Federal Aviation Administration, Washington, DC

1. INTRODUCTION

The purpose of this paper is to communicate the findings of an investigation into the differences between the National Weather Service's (NWS) Echo Tops Product (ET-P) and the Lincoln Laboratory's (LL) High Resolution Enhanced Echo Tops Product (HREET-P). Both products derive from measurements made with the NEXRAD WSR-88D meteorological radar system. The motivation relates to interests of the FAA's Enhanced Traffic Management System (ETMS) to provide the best weather information possible to its user community. The term Echo Tops (ET) is defined by the National Climatic Data Center (NCDC) as:

> The height of the greatest (in altitude) non-zero reflectivity value (greater than the minimum significant reflectivity, 18.5 dBZ) for each 4 x 4 km (2.2 x 2.2 nm) grid box on the surface of the earth.

The ET-P is one of forty-one (41) Level III NEXRAD products that are generated and made available in near real time to users of the NEXRAD system; archived data are also available from the NCDC. NEXRAD data for public use are categorized as Level II and Level III. Level II data are the three meteorological base data quantities: reflectivity factor, mean radial velocity and spectrum width. Level III data consist of interpretive, meteorological products that are derived from Level II data. Level II products are also available in near real time to users throughout the country for weather surveillance, forecasting and other applications, including the generation of specialty products for various applications including aviation operations and planning. The HREET-P is generated by the LL from Level II NEXRAD products in support of the Corridor Integrated Weather System (CIWS). It should be noted that both ET-P and HREET-P produce only estimates of actual Echo Tops because of the nature of scanning strategies that necessarily limit each radar's volume coverage. Comparison of ET-P and HREET-P to actual Echo Tops would best be made through simulations based on actual high-resolution RHI profiles of various types of storms obtained from research radars. Accordingly, the results presented here are limited to a comparison between the products of the ET-P and HREET-P algorithms.

* *Corresponding author address:* Thomas A. Seliga, DTS-53, Volpe National Transportation Systems Center, 55 Broadway, Cambridge, MA 02142; e-mail: seliga@volpe.dot.gov.

2. BACKGROUND

NEXRAD ET products have important utility for air traffic operations and management of the National Airspace System (NAS). The NWS legacy algorithm produces a single radar 4-by-4 km gridded product in 5-kft height increments up to a maximum height of 70-kft out to a range of 230-km. The product is derived from an estimate of the height of 18.5-dBZ reflectivity factor contours. The derivation of ET is dependent on NEXRAD radar volume coverage, which is necessarily limited because of the inherent nature of weather radar echoes and their impacts on sampling times, spatial coverage and spatial resolution. The legacy ET algorithm interprets the 18.5-dBZ threshold (or highest height of echoes that equal or exceed this value) as the echo top, while the LL algorithm uses a linear interpolation of reflectivity factor between adjacent elevation angles to estimate the height of the 18-dBZ reflectivity factor. Both products round ET values up to the next nearest height, i.e., ET-P to the next 5-kft level and HREET-P to the next 1-kft level. The LL ET product has higher spatial and temporal resolution as well. Results are generated in approximate gridded horizontal 1-by-1 km cells with 1-kft height resolution; the individual radar product extends out to a range of 345-km note that the available HREET-P values were in 2-by-2km cells. The legacy update rate for the national mosaic (composite or combination of data from all or a set of NEXRAD radars into a single product covering larger areas of interest than that of a single radar) used by ETMS is 5-min, while the LL CIWS mosaic is 2½ -min. Both ET products are reported relative to mean sea level (MSL). Since individual NEXRAD radars operate asynchronously, each ET product will differ somewhat depending on the way it accommodates updates from the radars. The nature of the two algorithms, as reported by LL, is illustrated in Fig. 1.

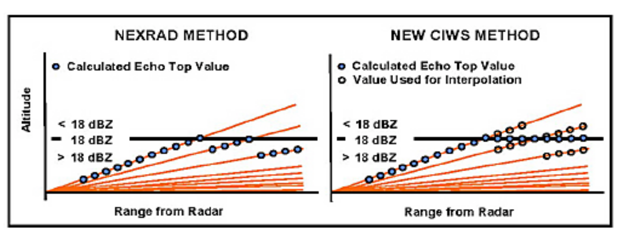

Fig. 1. Illustration of the methodologies of generating ET using the NWS and LL algorithms. http://www.ll.mit.edu/AviationWeather/EET-flyer.html

2.1. Basic Concepts

The comparisons between ET-P and HREET-P involve both qualitative and quantitative assessments. Qualitative comparisons are based primarily on images and plots of the products, while the quantitative comparisons rely mostly on statistical measures. The evaluations are limited to two common regions of spatial extent that offered potential for comparing somewhat different weather regimes. Complete CONUS comparisons were not possible because of the current, limited domain of the LL CIWS coverage and the LL inclusion of Canadian radars in its CIWS products. Although ET-P covers the CONUS, it does not include data from Canadian radars. The results indicate that images of both products are in general very similar with effects of spatial resolution differences being most noticeable near the edges of storms. The consequence of the different update rates is also evident in the images. Differences in clutter filtering at lower altitudes near the radars and effects of possible anomalous echoes due to high-flying aircraft in both products are also apparent. The statistical results for the mean echo tops over extended coverage areas are consistent with expectations resulting from consideration of the differences in the two algorithms.

2.1. Data Resources and Analysis

The ET data have been collected and archived starting in early 2005. The HREET-P data were acquired from the LL NEXRAD-based CIWS products via direct internet access in network Common Data Format (netCDF), and the ET-P data from the Enhanced Traffic Management System (ETMS) weather product suite provided by WSI in run-length encoded format. The findings described here are based on information obtained from analyses performed with a MATLAB-based Echo Tops Analysis Tool designed and developed for this application.

The data archive, consisting of CONUS reports on ET-P and CIWS reports on HREET-P cover the periods shown in Table 1. Five cases from this archive were selected for investigation and the comparisons. The dates included: Jan 3 & 13; Feb 14; and Mar 7 & 8.

2.2. Common Coverage Areas

Since the two ET products cover different regions of space, it was necessary to select one or more common areas for the comparisons. Furthermore, because of the matrix array formats of both data sets, it was convenient to make these common areas rectangular in shape. To ensure commonality, two different areas were selected for the comparisons. These were based on LL recommendations that would ensure commonality to both ET-P and HREET-P, that is, exclude regions affected by contributions from Canadian radars and restrict ET-P to the CIWS coverage area. The selected areas are identified by the green and blue boxes marked S and R, respectively, in Fig. 2.

DATES (2005)	ET-P	HREET-P
04 Jan to 16 Feb	X	X
22 Feb to 04 Apr	X	X
02 May to 30 Jun	X	X
01 Jul to		

Table 1. Data Archive of the NEXRAD-Based NWS Legacy ET-P and Lincoln Laboratory HREET-P Echo Tops Products.

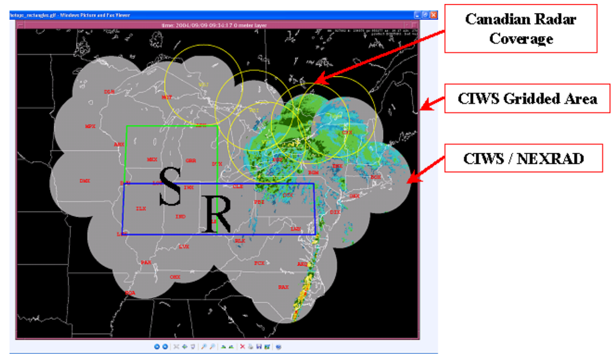

Fig. 2. Common areas used for comparative analyses of the NWS legacy Echo Tops ET-P and LL High Resolution Echo Tops HREET-P.

2.3. MATLAB Analysis Tool

To assist in making the comparisons between the two ET products, MATLAB-based tools were devised to read data, perform spatial filtering, produce and display graphics and plots and perform computations of statistical parameters. The capabilities include:

1) Data File Selection
- Choice of the appropriate LL or NWS data files for analysis

2) Area Selection Analysis for Display
- Selection of CIWS radar coverage area
- Selection of LL radar coverage area
- Selection of S or R coverage area

3) Statistics
- Histogram of both LL and NWS and derived metrics
- Statistical Parameters of both LL and NWS
  - Maximum (kft)
  - Mean (kft)
  - Median of (kft)
  - Standard Deviation (kft)
- Echo Tops (percentage of selected area with ET > 0-kft)
- Cumulative Distribution Function (CDF, and 1-CDF) for display

4) Video Playback
- Play Audio Video Interleave (AVI) of video files of sequences of ET images

5) Slices -Latitude and Longitude
- Selection of Longitude of the slice

- Selection of the range of Latitudes of the plot
- Selection of the location of the plot
- Selection of Latitude of the slice
- Selection of the range of Longitudes of the plot
- Selection of the location of the plot

6) Plot Selection (other)

- Difference Plot (image or plot of the difference between NWS ET-P and LL HREET-P values
- Contour Fill Plots (contour-filled image of ET)
- ETMS Representation (graphical image of the highest ET values in designated 200x200-km gridded areas that are currently available to ETMS users)
- LL Equivalent (same 200x200 product based on LL ET values)

7) Image Color Options

- Image Color Bar (entry from list of prescribed colormap formats used for the ET images and their associated colorbars)

2.4. Data Transformation

Since the two ET products are in different geographical spatial resolutions, it was necessary to reconcile this difference prior to performing any analyses or producing any images of ET. This process was designed to for compatibility with the MATLAB Mapping Toolbox functionalities. Thus, both data sets were transformed into Regular Matrix Map formats that are of equal size that maintained the effective spatial resolutions of each ET product.

A Regular Matrix Map is defined as a matrix of spatially dependent data that correspond to points or locations on a geographical grid at equiangular (equal-angle) intervals in both latitude and longitude. The Map contains columns of data running south to north and rows of data running west to east with each matrix element representing the same angular step in each direction for all rows and columns. A Map Legend defines the parameters of the Regular Matrix Map. It is a vector that identifies the geographic placement and unit cell size of the Regular Matrix Map. These parameters along with the size of the Regular Matrix Map define the geographical area (latitudinal and longitudinal extents) of the data contained in the Map.

First, the NWS ET-P were extracted from the NWS CONUS ET-P in order to conform as closely as possible to the geographical latitudinal and longitudinal limits of the LL HREET-P. Since the finest resolution of the two data sets corresponded to approximately 2-by-2 km cell sizes, the 0.0181 data points per degree latitude was selected as the Regular Matrix Map scale factor. The corresponding resolution size of a cell near the center of the geographic area of interest is approximately 1.5-by-2.0 km (WE-by-SN).

Resizing of the data sets was accomplished with the MATLAB *resizem* function. This function selects the nearest neighbor values for the data entries in the resized matrix. A key feature of this process is its ability to retain original values of the data while retaining their respective scaled locations in space.

3. COMPARATIVE IMAGES OF HREET-P AND ET-P

Fig. 3 illustrates two images of ET derived from the LL and NWS ET products, HREET-P and ET-P, respectively. The images cover the entire common area of the data sets for the time 1205 UT on March 7, 2005. It should be noted that HREET-P data do not cover the western-most and southern-most areas of the CONUS. Also, HREET-P includes data from Canadian radars near the US-Canadian border that are not included in ET-P. The impact of these two differences in the images is clearly evident. Another distinctive difference in the images is the obvious presence of very low altitude ET products in the ET-P image that are scattered throughout much of the coverage area. These ET values are attributed to ground clutter near the radars that has not been filtered out of the NEXRAD data used to generate ET-P. Since there is little evidence of such clutter effects in the HREET-P image, it appears that the LL algorithm effectively deals with this source of error in ET. Aside from these differences in the images, the two products are in general very similar in appearance. In particular, for ET values above a 5-kft, it appears that either one could be used to effectively portray both the location of significant storms as well as the height to which they reach in the atmosphere.

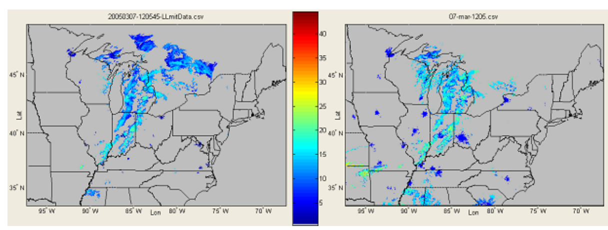

Fig. 3. Comparison of images of Echo Tops obtained from HREET-P (left) and ET-P (right) over their respective spatial domains.

3.1. Square Common Area (S)

Fig. 4 is a set of images covering the square (S) common area and using the same data shown in Fig. 3. There is good general agreement between the two images, although a number of differences are clearly discernible. Differences in the vertical resolution of HREET-P (1-kft) and ET-P (5-kft) are seen more clearly than in Fig. 3; that is, the finer discretization of HREET-P produces a smoother image as values transition in height compared to ET-P. The effects of ceiling the estimates of the two products (HREET-P to the next highest 1-kft level, and ET-P to the next 5-kft level) can also be seen; i.e., there is an inherent filled contour appearance to ET-P at discreet levels separated by 5-kft intervals that contain values of HREET-P that fall within the next lowest 5-steps of HREET-P (e.g., the yellow 15-kft ET-P levels in the image on the right nearly match the 11-to-15-kft, blue-green to yellow regions of the image on the left). The effects of clutter are more evident in the ET-P image on the right (blotches of blue); these are most evident near to the radars and are by-and-large missing from the HREET-P image on the left, suggesting that the HREET-P algorithm employs an effective means for filtering out such clutter from the data. However, close examination of the two images indicates that that the HREET-P clutter removal algorithm is not perfect; the presence of residual clutter effects are likely present in isolated areas near pixel values of (Lon; Lat) = (440; -375) and mixed with weather near (Lon; Lat) = (625; -370).

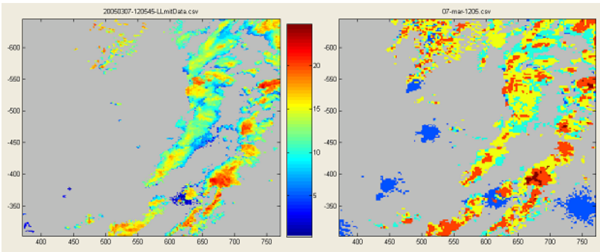

Fig. 4. Comparison of images of Echo Tops obtained from HREET-P (left) and ET-P (left) over the square common area designated by S in Fig. 2.

Another feature of interest is the rectangular region bounded on the corners by pixels (Lon; Lat) = (450; -550) and (600; -650). This region is considerably denser in values of ET-P compared to HREET-P. One possible reason for this difference is that clutter filtering in the HREET-P algorithm may have resulted in inadvertent removal of actual weather echoes. In this case, ET values up to 20-kft might have been affected/removed. Another difference in the images is the different extent of ET reports in certain areas; the region centered around (Lon; Lat) = (625; -450) shows much greater WE-extent in the HREET-P image, while the region centered around (Lon; Lat) = (620; -620) shows an opposite effect with the ET-P image being more extended spatially than HREET-P. Note also that just to the SW of this area, ET-P shows a region of ET that reaches 20-kft while HREET-P does not indicate any ET at all.

3.2. Rectangular Common Area (R)

Fig. 5 is a set of images covering the rectangular (R) common area of Fig. 2,c again using the same data presented in Fig. 3. Although less evident in Fig. 4, it should be noted that both the S and R images in Figs. 4 and 5 are not scaled geographically. Most of the same comments that were applicable to region S in the previous section apply, i.e., the discretization effects, removal of clutter and general good agreement are evident. In this case, there are no significant areas where ET appear on one and not the other, except where apparent clutter effects producing low values of ET-P.

A notable difference is indicated, for example, in the ET-P image at approximately pixels (Lon; Lat) = (1040; -432) where there is an isolated report of 20-kft ET with no corresponding report in HREET-P. This difference is attributed to ET-P reporting false weather echoes arising from the corresponding NEXRAD radar detecting aircraft with no effective means employed to recognize such false echoes and removing them from the data. This effect is more prevalent on images of ET-P than on those of HREET-P, suggesting that the LL ET algorithm includes more effective means for detecting and removing false echoes due to aircraft than the NWS algorithm.

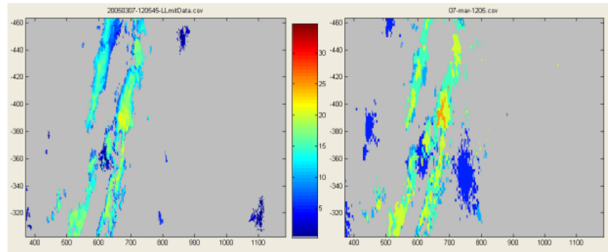

Fig. 5. Comparison of images of Echo Tops obtained from HREET-P (left) and ET-P (right) over the rectangular common area designated by R in Fig. 2.

3.3. Difference Images

The Difference Plot feature on the MATLAB analysis tool is useful for displaying an image of the difference in the ET-P and HREET-P images on a cell-by-cell basis. The difference image [HREET-P less ET-P] associated with the two images in Fig. 3 is shown in Fig. 6. Thus, positive values signify regions where HREET-P is greater than ET-P, and negative values regions where ET-P is greater than HREET-P. The different coverage of the CIWS- and NWS-based ET products is readily apparent, as is the inclusion of Canadian radar measurements in HREET-P. In conformity with the different ceilings/resolution of the two data sets, most of the common areas differ typically between –5-kft to +5-kft. Edge-type effects are also present; these may be due to small differences in the spatial resolution of the two data sets, differences in their spatial registrations and the different update rates of the products (ET-P every 5-min and HREET-P every 2.5-min).

The square region S of the difference image in Fig. 6 was extracted to produce the difference image shown in Fig. 7. Note that the color scale in this figure differs from that in Fig. 6. This image again illustrates (with better spatial resolution) the characteristics previously noted, including the presence of clutter in ET-P, the possible inadvertent removal of weather data by the LL algorithm, edge effects attributed to differences in spatial resolution, differences in spatial registration and different update rates.

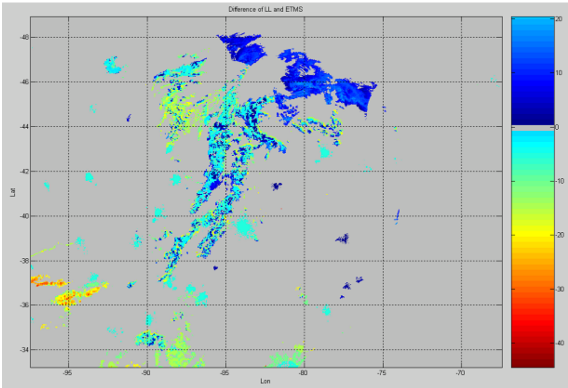

Fig. 6. Difference image of the HREET-P and ET-P images in Fig. 3. [HREET-P less ET-P]

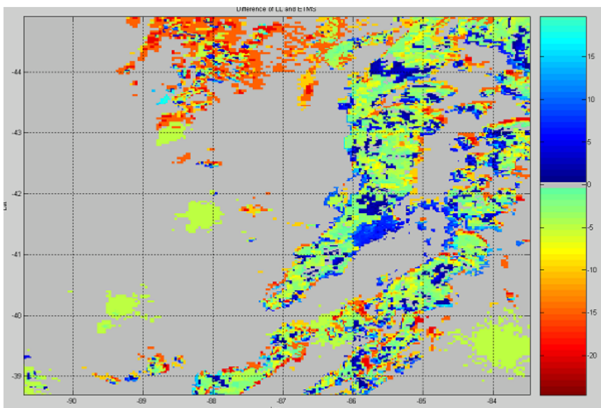

Fig. 7. Extracted difference image of the HREET-P and ET-P image in Fig. 6, corresponding to the square common region S shown in Fig. 2. [HREET-P less ET-P]

3.3 Longitudinal and Latitudinal Slice Plots of ET

A more quantitative sense of the similarities and differences in the two ET products can be seen by examining superimposed plots of ET-P and HREET-P along longitudinal and latitudinal slices of their respective images. Examples of these are shown in Figs. 8 and 9 for data extracted in the common square area S. Fig. 8 compares the products along a slice extending west to east from around -88.4^{o} to -83.8^{o} longitude at latitude of 40.4^{o}. Values of –1 on the HREET-P plot are actually 0-kft; the –1 value is used by LL to indicate the coverage areas of the radars used to derive the ET product. There is good general agreement between both products with the different vertical resolutions being readily apparent, ET-P in 5-kft steps and HREET-P in 1-kft steps. The effects of ceiling the products are also easily seen, particularly in ET-P. There is a maximum difference in the two of ~5-kft at -85.2^{o} longitude. In this case, HREET-P just reaches 20-kft, and ET-P takes on values of 25-kft. Differences in the spatial registration and/or effects of sampling rates of the two products may also be evident, particularly at the edges of the farthest west weather feature. It is easy to imagine storm motion being updated at the faster rate with HREET-P, displacing its plot eastward relative to the ET-P plot. The same feature is not seen in the east-most weather region of the plot, most likely because the update times of both products are the same in this region.

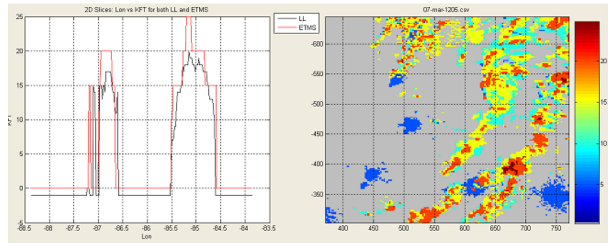

Fig. 8. Plot of HREET-P and ET-P along a longitudinal slice shown in the image of ET-P on the right. The corresponding image of HREET-P is given in Fig. 4. The value of –1-kft for HREET-P is used to signify radar coverage for the CIWS-based HREET-P.

A second example of a plot is shown in Fig. 9 for a latitudinal slice extending from 40.15^{o} to 42.05^{o} in latitude at a longitude of -84.4^{o}. Similar behavior to the longitudinal plot is seen in this plot. Of particular interest is the very good general agreement on the placement and spatial variation of the features of the products. However, the maximum differences are greater with ET-P exceeding HREET-P by as much as 8-kft at ~40.9^{o} latitude. Much larger differences are at just under 41.4^{o}, but these are most likely associated with sampling update differences, reflecting a southern movement of the weather feature at this longitude that would displace them in latitude relative to each other.

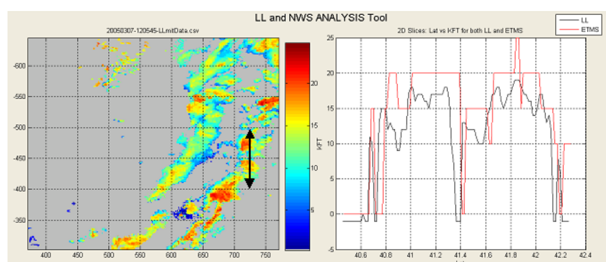

Fig. 9. Plot of HREET-P and ET-P along a latitudinal slice shown in the image of HREET-P. The corresponding image of ET-P is given in Figs. 4 and 8. The value of –1-kft for HREET-P is used to signify radar coverage or the CIWS-based HREET-P.

4.0 Statistical Comparisons of HREET-P & ET-P

Five cases were selected to determine the statistical differences between the ET products. The comparisons were based on data that had ET values greater than zero in the common regions of interest. The metrics included: histograms; means; medians; standard deviations; and the areal coverage in percent of the common area of interest. Differences in these metrics were also produced, based on [ET-P less

HREET-P]. Five cases were selected for analysis, corresponding to the five data set cases listed is Sect. 2.1.

Each case consists of five consecutive time samples of each product. Both the square S and rectangular R regions of the common coverage area of the ET products were included as were differences in the statistical parameters and averages of the differences for each case.

Interpretation of the results of the statistical analyses lead to the following set of conclusions:

1) The areal coverage with reported values of ET are greater for ET-P than for HREET-P, ranging from just over 0% in region R on 13 Jan to around 10% in region S on both 3 Mar and 8 Mar. Much of the added coverage is attributed to clutter being interpreted in terms of ET products in ET-P, while it is presumed that much of this clutter is detected and accounted for in HREET-P and thus excluded from corresponding ET reports.

2) The maximum values of ET-P and HREET-P are expected to be generally consistent with the expectation that ET-P are ceilinged to the nearest 5-kft interval while HREET-P are ceilinged to the nearest 1-kft interval. However, the differences will also be affected in the opposite direction by the interpolation of HREET-P to higher heights, leading to higher values of ET for this product in certain circumstances of radar elevation angles and reflectivity factor profiles. For the five cases examined, the average maximum difference between ET-P and HREET-P ranged from 0.8- to 8.0-kft for the basic 1-kft height resolution values of HREET-P and from –1.0- to 5.0-kft for the ceilinged HREET-P values.

3) Examination of the maximum ET values can also be used to detect instances of anomalous behavior. For example, on 13 Jan at 1405, the maximum HREET-P was 36-kft while the maximum ET-P was 30-kft. This outlier was seen in histograms of the data; otherwise, the results between the products would have been consistent. The image of HREET-P for this time is shown in Fig. 10. The outlier is most likely due to an aircraft radar echo that was not filtered out of the data by the HREET-P algorithm; its location is encircled on the figure. It is noted that this same outlier was not readily present in ET-P; this may be due to the different spatial resolutions of the two products, possibly leading to reduced intensity of the reflectivity factor used to determine ET-P by as much as 12-dB. Thus, an 18.5-dBZ 4-by-4-km average threshold value for ET-P could have easily been suppressed below this threshold, if the threshold were exceeded in the HREET-P 1-by-1-km resolution cell. This situation is discussed further in the next item.

4) One way of automating the detection of outliers is to examine the difference between the maximum and the mean. The difference can be used to detect the possible presence of high-flying aircraft in the region of interest affecting the ET results. In addition to the previous result in Fig. 10, another event apparently is present in both ET-P and HREET-P at 1320 on 3 Jan. In this instance, the maximum ET-P and HREET-P values are 50-kft and 48-kft. The corresponding mean values of these products are 17.7-kft and 15.3-kft, respectively. The normal difference in these products appears to differ by a factor of two, while in this one case they differ by about a factor of 2.9 for ET-P and 3.2 for HREET-P. The outliers for HREET-P and ET-P for this case are shown as being co-located in Fig. 11.

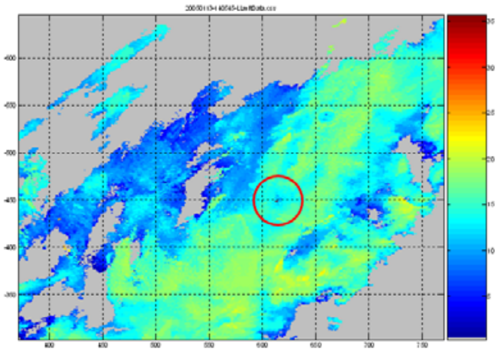

Fig. 10. 13 Jan at 1405: Location of an outlier high-altitude HREET-P value of 36-kft. The background weather products are typically less than 25-kft, suggesting that the high value is an anomaly resulting from detection of an aircraft that was not removed in the HREET-P algorithm.

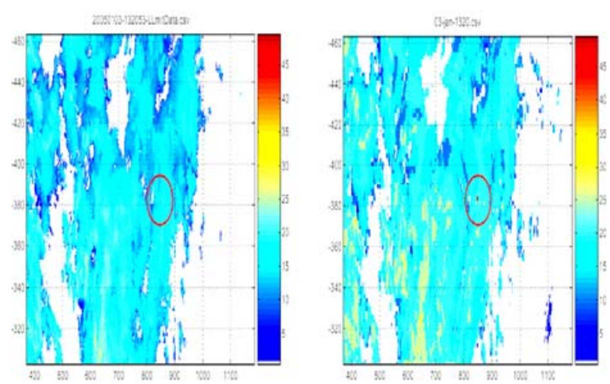

Fig. 11. 03 Jan at 1320: Location of the outlier high-altitude HREET-P (left) and ET-P (right) values at 48- and 50-kft, respectively. The background weather products are typically less than 30-kft, suggesting that the high values are anomalous, resulting from detection of an aircraft that was not removed in either the HREET-P or ET-P algorithms.

5) Absent effects of interpolation of HREET-P and for a uniform reflectivity factor distribution in any 5-kft ET interval, the mean of ET-P and HREET-P for uniformly distributed values of ET should differ by 2.0-kft with ET-P being larger because of the way

the reports are generated through ceiling of the data. In certain instances, interpolation should cause HREET-P to be greater, since HREET-P extends ET to higher heights (and also uses a lower 18-dBZ as the threshold) while ET-P treats the highest elevation angle reflectivity factor above 18.5-dBZ as the ET height (ceiling to the next highest 5-kft interval). The results show that the mean ET-P exceeds the mean high resolution HREET-P by about 0.4- to 2.4-kft, depending on the type of weather. Transformation of HREET-P to lower 5-kft resolution values by ceiling the 1-kft values to the next highest 5-kft interval produced mean differences of –1.8- to 1.4-kft. This latter result indicates that there is excellent agreement between the mean ET-P and HREET-P when both products are resolved to equal, lower resolution height resolutions.

6) The median of both ET-P and HREET-P are measures of the central tendency of their respective distribution of values. Half of the values are larger than the median value, and half are smaller. Comparing the median to the mean also indicates whether the distribution is skewed and in what direction it is skewed. For the five cases examined here, the average median of ET-P exceeded the median of HREET-P by –0.6- to 5-kft for the high-resolution HREET-P values and by –0.6- to 4.0-kft when HREET-P was transformed to the lower resolution 5-kft intervals. Comparisons of the median with the mean HREET-P indicate that the first two cases were predominantly skewed negatively, confirming that their distributions (histograms) with height are asymmetrical; this characteristic is clearly evident in the HREET-P histogram, but is notably less clear in the lesser resolution histograms for ET-P. The higher resolution histograms are clearly more useful for gleaning insights into the nature of the storms responsible for the ET reports as discussed further in Item 7 below.

7a) Histograms of HREET-P and ET-P provide useful insights into the height distribution of the values of ET in the area of interest. They also reflect the nature of the storms being examined. The HREET-P histograms are clearly much more revealing of storm structure than those of ET-P. As noted previously in Item 6 above, the loss of height resolution is readily seen from both the comparisons of the histograms of HREET-P with ET-P and comparisons of high-resolution HREET-P with low-resolution HREET-P histograms (Fig. 11).

7b) Significant skewness in the HREET-P histograms is readily detected as are suggestions of bimodal behavior. The former was discussed when comparing the median and mean previously in Item 7a above. The latter bimodal behavior is clearly evident in the second case on Jan 13. This is illustrated in the histogram of HREET-P for the time 1420 as shown in Fig. 11. Note that the resolution of the corresponding histogram for ET-P does not readily reveal this same behavior. Therefore, the results appear characteristically different for the two ET products. HREET-P clearly shows the presence of bimodal behavior that is most likely due to different type of storms being present in the common area of interest. There are two peaks in the HREET-P distribution, the lowest one around 10-kft and the highest one at 16-kft. The lesser resolution of ET-P masks this bimodal feature, which can have important consequences for aviation applications such as air traffic management and nowcasting of storms, based in part on ET data. Demonstration of the bimodality was simulated by a bimodal normal distribution of Echo Tops with peaks at 10- and 16-kft and standard deviations of 2.9- and 1.55-kft, respectively. The results are shown in Fig. 12. The distribution consists of an equal number of data points used to generate the HREET-P histogram in Fig. 11. There are also an equal number of data points in each bimodal component of the total distribution. The resemblance to the actual histogram in Fig. 11 is striking. The result demonstrates the utility of employing high-resolution HREET-P histograms or sampling distributions for detecting and characterizing ET-related weather activity.

In order to test the above different storm type hypothesis, images of HREET-P and ET-P are shown for this time in Fig. 13. Both the HREET-P and ET-P images show comparable areas being covered by ET values ranging from 0-to15-kft to areas ranging from 15-to25-kft values. In the square space S, there were:

~ 45,000 values of 0- < HREET-P <15-kft, and

~ 35,000 values of 15- ≦ HREET-P ≦ 25-kft.

The former values appear to be associated more with stratiform-type precipitation while the latter appear to be considered more convective. Note that perusal of the ET-P image would also reveal this bimodal behavior, although the corresponding histogram masks this property of the image!

8) The standard deviation (STD) of ET-P and HREET-P should be nearly equal with STD of ET-P being typically slightly greater due to the higher ceilinged values occurring at the highest ET in the distribution. The STD difference ranges between 0.4- to 0.8-kft. When HREET-P is transformed to lower resolution values, the difference is 0.1- to 0.9-kft.

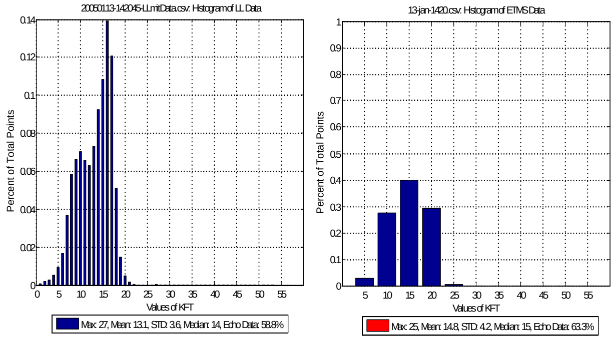

Fig. 11. Histograms of HREET-P (left) and ET-P (right). Bimodality is clearly evident on the high-resolution HREET-P, which appears to be masked on the low-resolution ET-P histogram. The bimodal peaks are at approximately 10- and 16-kft.

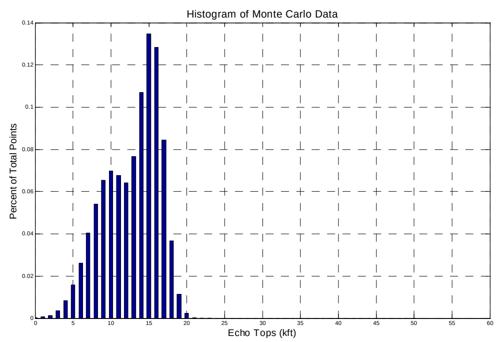

Fig. 12. Histogram of simulated bimodal normal distribution of ET with peaks at 10- and 16-kft and standard deviations of 2.9- and 1.55-kft, respectively. The number of data points matches the data points in the HREET-P result in Fig. 11.

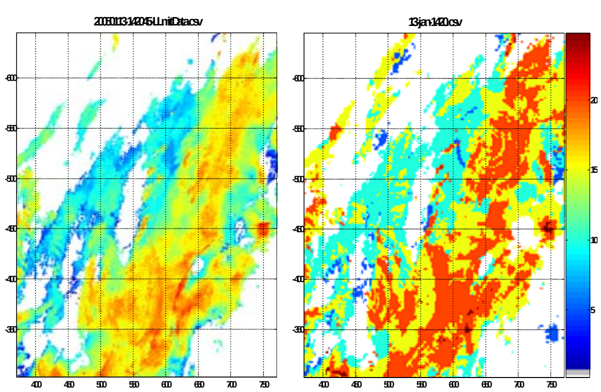

Fig. 13. 13 Jan at 1420: Images of HREET-P (left) and ET-P (right) corresponding to the presence of bimodal behavior of HREET-P in the histograms of ET in the common S region. The bimodality is clearly evident on both images even though the ET-P histogram seems to mask this phenomenon. The images are also useful to illustrate the well-known ring-type artifact in the ET-P values due to the way the NWS algorithm uses the threshold to determine ET as illustrated in Fig. 1. Note that this artifact is not completely removed in HREET-P as discussed in 9).

9) The fact that ET-P is found from the highest height at which the reflectivity factor equals or exceeds 18.5-dBZ (as opposed to the actual height where it equals 18.5-dBZ) can produce well-known underestimates of ET. Under uniformly stratiform conditions and finite sampling with elevation angle, this can produce a characteristic zigzag pattern in the measurement of ET as illustrated in Fig. 1. The phenomenon is also dependent on scan strategies (Brown and Wood, 1999; Scott et al., 2003), since the sequence of elevation angles within a given volume coverage pattern (VCP) determines to a great extent the vertical resolution capabilities of the radars. Also, the reduced height resolution of ET-P will affect the product. The methodology used for HREET-P helps mitigate this effect by interpolating reflectivity factor data with height to estimate the height of the threshold value; using higher height resolution (1- vs 5-kft intervals) also reduces the effect. The zigzag effect is evident in the ET-P image in Fig. 13. They appear as concentric-type rings around a radar. In this S area, as many as four sets of rings can be seen associated with the NEXRAD radar coverage in the area. By and large, these artifacts are mostly missing in the HREET-P image, although some evidence of rings is present several places on the image. Two easily identified large HREET-P rings, located around pixel coordinates (590, 375) and (620, 390) are concentric with ET-P rings. The enhanced values range from 1-to 3-kft over adjacent ET values. As opposed to the ET-P rings, which are prominent at nearly all distances from the radars in this instance, the HREET-P rings appear more prevalent at the farthest distances. The reason for these rings has not been ascertained. Contributing causes may, among other factors, relate to: the process used to combine radar data to form a mosaic; the way in which the interpolation is applied under certain spatial patterns of reflectivity factor; the distance from the radar; and possible effects of different beam-filling patterns. The important result here is that the HREET-P algorithm can also produce concentric, but less evident, rings centered around a given radar. In this case, the maximum deviation produced an apparent increase of ET up to a maximum of around 3-kft.

VIP	1	2	3	4	5	6
Level	1	2	3	4	5	6
dBz	18- 30	30- 38	38- 44	44- 50	50- 57	>57
Rate	L	L M	M H	H	VH HL	VH HL LHL

Table 2. VIP levels that have been used to traditionally contour radar reflectivity factor (dBZ). L – Light Rain; M – Moderate Rain; H – Heavy Rain; VH – Very Heavy Rain; HL – Hail; LHL – Large Hail.

5. PHYSICAL INTERPRETATION OF ECHO TOPS

The choice of 18.5 dBZ (18 dBZ) as the threshold for determining Echo Tops is consistent with the lowest reflectivity factor associated with the first of six Video Integrator and Processor (VIP) Levels that have been used to traditionally contour radar reflectivity factor (dBZ) as indicated in Table 2.

Both the 18.5 and 18 dBZ thresholds for ET used by the NWS and LL, respectively, reflect this choice of VIP-1 as the threshold. That is, the base threshold for Level-1 has been taken to represent the transition boundary from significant weather at lower altitudes to insignificant weather at higher altitudes. This VIP-1 Level can also be referred to rainfall rate, using the stratiform rainfall Marshall-Palmer (MP) formula.

$$Z = 200R^{1.6} \tag{1}$$

where

$$Z(dBZ) = 10\log(Z) \tag{2}$$

Z is reflectivity factor in mm^6-m^{-3} and R is rainfall rate in mm-h^{-1}. At 18.5-dBZ, the MP rainfall rate is 0.52-mm-h^{-1} or 0.021-in-h^{-1}. Alternatively, the NEXRAD default Z-R relationship,

$$Z = 300R^{1.4} \tag{3}$$

(which is a compromise between stratiform and convective rainfall) yields values of R at 18.5-dBZ of 0.41-mm-h^{-1} or 0.016-in-h^{-1}.

It should be noted that the choice of VIP-1 as the threshold for ET is associated with expectations of significant weather being based on the assumption of the radar observing rainfall. That is, the use of the VIP-1 level is more appropriate to base reflectivity factor measurements (dBZ values derived from rainfall at the lowest elevation angle scan of the radar). In contrast to this reference, its use for ET should account for the fact that under most circumstances the radar would be observing scattering from ice particle hydrometeors as opposed to raindrops. If the assumption of VIP-1 is valid, then the ice phase implication can be significant for determining ET heights when the threshold is applied to air traffic operations and management. Another factor in this regard is the fact that significant turbulence is known to occur often when aircraft enter space with reflectivity factors as low as 15-dBZ or less.

The above discussion implies that consideration should be given to altering (i.e., reducing) the ET reflectivity factor threshold for determining minimum safe flight levels, especially when ET is used for enroute operational guidance. The recommended change could still retain the reference to VIP-1 while simultaneously reflecting the fact that at high altitudes the radar most often responds to scattering from ice particles instead of raindrops. The result would also be consistent with the fact that significant turbulence, which can be severe, is often present in high-altitude regions with reflectivity factors less than 18-dBZ. The approach to establishing this recommended threshold is to replace the NWS 18.5-dBZ level by its equivalent value that would result from scattering from spherical ice phase hydrometeors having the same water content as raindrops producing a reflectivity factor of 18.5-dBZ. For pure spherical ice hydrometeors, the suppression in reflectivity factor that would be seen by a weather radar is approximately 6.5-dB, which means that the rainfall-based VIP-1 threshold of 18.5-dBZ equates to an ice-based threshold of 18.5-dBZ less 6.5-dB or 12-dBZ. Thus, if the VIP-1 threshold is valid, this implies that 12-dBZ may be a more reasonable threshold from which ET should be derived, particularly if ET are given in 1-kft intervals. Experimental confirmation of this threshold could be readily tested and evaluated by monitoring turbulence experienced by aircraft flying over storms at different heights relative to ET heights obtained with different reflectivity factor thresholds.

6. CONCLUSIONS AND RECOMMENDATIONS

This study performed qualitative and quantitative comparisons of the Echo Tops (ET) products generated by the NWS and LL NEXRAD-based algorithms. Values of ET, derived from the legacy NWS algorithm (designated as ET-P) have been used by the FAA's Enhance Traffic Management System (ETMS) while the LL ET product (designated as HREET-P) has been devised as an enhanced product for use in the FAA's Corridor Integrated Weather System (CIWS). Basically, HREET-P has 1-kft vertical resolution and 1-by1-km cell or pixel sizes (HREET-P data used here had 2-by 2-km), while ET-P has 5-kft vertical resolution and 4-by 4-km cell or pixel sizes. The most significant findings are outlined below.

6.1. Echo Tops Images

Images of ET-P and HREET-P were in general very similar in form and content. The higher resolution of HREET-P could be readily seen and is clearly superior in this regard. Both products were found to contain apparent false weather echoes that were most likely due to aircraft that were not adequately filtered out of the base NEXRAD reflectivity factor products (or the derived ET products). ET-P obviously included effects of clutter that often typically produced false ET values of 5-to 10-kft over extensive areas; these values were most evident near the radar locations. Most of these effects were missing from HREET-P; this was corroborated by the statistical analyses which included a measure of areas having ET greater than 0-kft for each product. It is apparent that HREET-P is more effective in removing clutter effects, although an instance of possible loss of weather data was observed that might have been due to inadequacies in the clutter filtering. Instances of apparently false high values of ET were discovered in both ET-P and HREET-P, which, if used without effective means of determining their representativeness of real weather or indicating the locations and size of the areas affected, could lead to significant incidences of false reporting of high ETs over affected portions of the CONUS. It is noted that it is also possible that many of the apparently false ET reports due to aircraft echoes may actually be weather-based. For this to occur, they would have to be single, isolated, highly convective thunderstorms covering very small areal extents. The NEXRAD reflectivity factor database should be more than adequate to make such determinations to ensure integrity of the apparently anomalous ET values.

6.2. Plot Comparisons

The analytical procedures included a capability to compare longitudinal and latitudinal slices of HREET-P and ET-P data. Examination of numerous plots indicated that the results were very much in good qualitative agreement with each other. The plots display both the differences in vertical resolution as well as probable effects due to different sampling update rates (5-min for ET-P and 2.5-min for HREET-P). Occasional significant differences in heights were detected, amounting to as much as 10-kft.

6.3. Statistical Properties

A limited grouping of statistical parameters of ET-P and HREET-P were computed for a set of five events on different days over two areas (designated S and R) common to both products. These consisted of: the percentage of the common areas reporting ET values greater than zero; the maximum, mean, median and standard deviation of ET; and normalized histograms or sample distributions of values greater than zero. The percentage areas were considerably greater for ET-P, most likely due to lack of effective removal of clutter by the NWS legacy algorithm compared to the LL algorithm. The maximum values were often attributed to a single or few pixels; they appeared to be due to aircraft echoes that were not properly removed from the NEXRAD reflectivity factor database, although this was not confirmed.

The average difference between the means of ET-P and HREET-P were consistent with expectations, based on the different vertical resolutions, how the algorithms ceiling the data, how the thresholds are applied and the slight difference in the threshold values. Median values were used to compare with mean values to determine skewness in the distributions of ET for each product. This property was also observed by examining the histograms, which consistently showed dominance of negative skewness for those sample events which contained large areas of convection as judged from ET images. This implies that high-resolution histograms can be used to detect the presence of significant convective weather. Absence of values at levels greater than around 10-kft are readily evident in the images and histograms and appear to be indicative of stratiform weather conditions.

The high-resolution 1-kft histograms of the presence of two storm types (stratiform vs. convective); this feature was readily apparent in one set of HREET-P histograms. The same time reduced resolution histograms of ET-P masked this important statistical property. A clear case of bimodality was easily modeled by simulated data.

6.4. Ring Effects

Because of the way the reflectivity factor threshold is applied in the ET-P algorithm (equates ET to highest height in a radar volume scan where reflectivity factor equals or exceed 18.5-dBZ), ET values will be range-dependent, appearing as a zigzag pattern as illustrated in Fig. 1. The effect on an ET image can cause the image to have an appearance of rings centered about the radars. A clear example of this was shown and compared with the same-time HREET-P image. Interestingly and unexpectedly, the HREET-P image also showed ring behavior. <u>Two large HREET-P rings, each associated with different radars, were easily identified as being concentric with ET-P rings.</u> The enhanced values of HREET-P relative to adjacent areas near the rings ranged from 1-to 3-kft. As opposed to the ET-P rings, which are prominent at nearly all distances from the radars in this instance, the HREET-P rings appeared more prevalent at the farthest distances. The reason for these rings has not been ascertained. Contributing causes may, among other factors, relate to: the process used to combine radar data to form a mosaic; the way in which the interpolation is applied under certain spatial patterns of reflectivity factor; the distance from the radar; and possible effects of different beam-filling patterns.

6.5. Physical Interpretation of the ET Products

The reasoning behind the choice of 18.5-dBZ and 18-dBZ as thresholds for the ET products was examined. It is apparent that the choice was related to VIP levels used to classify weather radar echoes. The first Level-I traditionally represents weather that produces reflectivity factors between 18-30-dBZ and is meant to signify light precipitation conditions. The threshold was examined in terms of ice-type hydrometeor conditions most appropriate to the highest levels in storms compared to water-phase precipitation for which the VIP levels usually apply. It was shown that, if the condition of light precipitation is an appropriate threshold for determining ET, then the 18- or 18.5-dBZ threshold should be altered to reflect ice hydrometeor conditions. Since the reflectivity factor of spherical ice phase hydrometeors having the same water content as the same distribution of water droplets would be smaller by around 6.5-dB, the equivalent VIP Level threshold would be reduced to 11.5- or 12-dBZ, depending on choice of threshold value employed. It is not known whether the higher values of ET that would result from such a change in the threshold would be more appropriate for aviation. This is an important issue for aviation and its use of ET data in the operational management and control of air traffic in adverse weather conditions.

6.6. Recommendations

The results of this investigation were used to formulate a set of recommendations for consideration by the ETMS community and possibly others with interests in ET products. These are classified into two types: primary, for immediate consideration for ETMS; and, general, for longer term potential by ETMS and others within the meteorological community.

Primary

HREET-P is clearly superior to ET-P. Nevertheless, the latter produces very good and useful products (ET-P) that should continue to be used until such time that the HREET-P is available as a NEXRAD Primary Level III Product that covers the entire CONUS. Since each NEXRAD radar has already implemented the HREET-P for local use, the NWS Radar Support Facility should replace the current ET-P product by the HREET-P. The statistical comparisons in this study show that results similar to the current ET-P can readily be derived from the HREET-P, thereby mitigating against any concerns that the new product might significantly affect long-term use of ET-P as archived products possibly used by others in climatology or other areas such as a factor in developing or testing nowcasting algorithms.

The ETMS use of alphanumeric maximum values of ET within gridded 200-by 200-km regions should be replaced with an appropriate graphical representation that displays the spatial distribution of the product. False color images, combined with contouring seem most appropriate, and these may be usefully supplemented by alphanumeric products and other graphics derived from the statistics of the ET product. The implementation of this new ET product(s) for ETMS should be capable of ingesting HREET-P data whenever this product has been certified and made available as a replacement for ET-P as the Primary Level III NEXRAD Product.

Studies into the preferred imaging and contouring features of ET products are required to establish the most useful image formats for ETMS users.

General

The presence of apparent anomalous values of ET that appear due to the presence of aircraft echoes in the NEXRAD data needs further exploration to test this hypothesis. Access to NEXRAD Level II data would be needed for this task to examine the vertical profiles of reflectivity factor in the vicinity of the anomalous reports.

The relatively limited amount of statistical analyses performed in this study, including generation of histograms, suggests that a number of different forms of alphanumeric descriptions might also prove useful for National Airspace System (NAS) management and operations. This concept should be explored more fully. Concomitant with this should be investigations into product definition and the means of communicating them to users.

The study was significantly limited in that only comparisons between the products of two different algorithms could be performed. Since the NEXRAD radars are necessarily limited in their ability to provide complete volume coverage as well as in their spatial resolution, it is not possible to determine how well either product compares with actual ET values based on the actual ET heights. Both products should be examined relative to such values in order to establish their true accuracy limitations relative to actual ET values. The approach should preferably utilize simulations derived from high-resolution reflectivity factor profiles obtained in different types of storms with high spatial resolution research radars.

The apparent VIP-basis for the 18-/18.5-dBZ ET thresholds should be examined relative to its impact on aircraft safety and turbulence. Given the existence of a considerable NEXRAD ET database and the availability of real-time ET products, a research program could readily be designed to answer related questions.

The imaging of ET products, statistical analyses and properties of the product and their time history are strongly suggestive of the product's importance for gauging storm intensity, tracking storms and weather nowcasting. Numerous related concepts, including how to combine ET data with other radar, satellite and atmospheric data for optimization weather information for this purpose should be explored.

7. ACKNOWLEDGMENTS

This study was performed in support of the FAA Air Traffic Organization System Operations Services (ATO-R). The cooperation of Randy Steadham of the National Weather Service Radar Support Facility and the MIT Lincoln Laboratory team of people responsible for the development and operational production of various aviation-based weather products used in the Corridor Integrated Weather System (CIWS) that includes HREET-P is greatly appreciated. David J. Smalley of LL was especially helpful in providing valuable insights and access to NEXRAD-based CIWS products. The NWS ET-P data were taken from ETMS records derived from the legacy Echo Tops product.

8. REFERENCES

Brown, R. A. and V. T. Wood, 1999: Development of New WSR-88D Scanning Strategies for Convective Situations, Final Report, Task 8.2, Memorandum of Understanding Between WSR-88D Operational Support Facility and National Severe Storms Laboratory, Norman, OK.
http://www.nssl.noaa.gov/~wood/OSF_MOU/CY98/Task 8.2/FinalReport.html

Scott, R., R. M. Steadham and R. A Brown, 2003: New Scanning Strategies for the WSR-88D, Preprints 19th Int. Conf. On Interactive Information and Processing Systems for Meteorology, Oceanography and Hydrology, Amer. Meteor. Soc., Long Beach, CA.

Smalley, D. J., B. J. Bennett and M. L. Pawlak, 2003: New Products for the NEXRAD ORPG to Support FAA Critical Systems, Preprints 19th Int. Conf. On Interactive Information and Processing Systems for Meteorology, Oceanography and Hydrology, Amer. Meteor. Soc., Long Beach, CA.